lubricants

MDPI

Article

The Performance of Carbon-Based Nanomaterials in Different Base Oils and an Oil Blend

Jack Nasr and Diana-Luciana Cursaru *

Faculty of Petroleum Refining and Petrochemistry, Petroleum-Gas University of Ploiesti, 100680 Ploiesti, Romania; jack@upg-ploiesti.ro

* Correspondence: dianapetre@upg-ploiesti.ro

Abstract: Different carbon-based nanomaterials (fullerenes, graphene, SWCNTs, and SWCNT-COOH) were tested as additives in a base mineral oil, SN150; rapeseed oil (RSO); and a 50/50 by volume blend of the two using an HFRR (high-frequency reciprocating rig) tester for coefficient of friction (COF) and wear scar diameter (WSD) determinations and a four-ball tester for welding point determinations. The concentrations considered for the HFRR tests were 0.1, 0.5, 1, and 2 wt.%, while the concentration considered for the welding point tests was 0.5 wt.%. The results of the welding point tests showed that the addition of different nanoparticles made it so that welding occurred at much lower pressures compared to the pure oils. This is due to the hardness of the nanoparticles, which increases the local temperature and pressure at the contact points between them and the surfaces, causing welding to occur much sooner. The results of the HFRR tests showed a possible synergistic effect between the fullerenes and SWCNT-COOH and the oil blend, which may be attributed to possible interactions that occurred at a molecular level between the nanoparticles and the different molecules of the oil blend.

Keywords: carbon-based nanoparticles; coefficient of friction; wear scar diameter; welding point; oil blends

1. Introduction

With the push towards "decarbonization" that parts of the world are currently experiencing and the goal being set for certain countries such as Germany to become climate-neutral by the year 2045, adequate environmentally friendly alternatives to existing mineral-oil-based products are undergoing research to verify their viability. This also holds true in the lubricants industry, where companies and researchers are actively looking for ways to reduce reliance on mineral oils and replace them with viable alternatives. Biodegradability is a key factor that should be considered when choosing an adequate alternative. As such, different kinds of vegetable oils (VOs) and oil blends have been proposed and are being continuously studied in order to determine their viability.

Aside from their high biodegradability [1], vegetable oils are well known for their high lubricity, and this is reflected well in many research papers that have been published over the years in which VOs outperformed mineral-based oils in terms of reducing friction [2–4]. However, VOs suffer from certain drawbacks, including their relatively low pour points [5] as well as their low oxidative stability [6]. These factors can be overcome, as some studies have shown that the addition of certain antioxidants can enhance the oxidative stability of VOs to levels comparable to commercially available lubricants [7,8].

Another potential option that is being considered is the usage of oil blends formulated using traditional mineral-based oils and vegetable oils. These blends can potentially bridge the gap between mineral and vegetable oils in terms of performance and limit their individual drawbacks. Jatropha, castor, palm, and soybean oils are some of the oils whose addition at low concentrations to mineral-oil-based lubricants showed noticeable performance improvements [9–12]. This could prove to be a more feasible approach towards

Citation: Nasr, J.; Cursaru, D.-L. The Performance of Carbon-Based Nanomaterials in Different Base Oils and an Oil Blend. *Lubricants* **2024**, *12*, 90. https://doi.org/10.3390/lubricants12030090

Received: 21 January 2024
Revised: 21 February 2024
Accepted: 8 March 2024
Published: 13 March 2024

reducing the usage of mineral-based oils by up to 50%, depending on the ratios of the oils in the blends.

Lubricants are not only composed of the base oils that comprise them; additives form an essential part of a lubricant formulation as they are employed to overcome the shortcomings of base oils and improve their performance for specific applications. These include viscosity modifiers, pour-point depressants, and extreme pressure and anti-wear additives, among others, which have been used in industry for decades. However, over the last two decades, another category of additives has been gaining increased relevancy: nanoadditives.

The effects of different kinds of nanomaterials on the performance of lubricants have been explored in an ever-increasing number of research papers. These nanomaterials range from metals such as Cu [13] and Ag [14] and metal oxides such as CuO [15] and ZnO [16] to carbon-based nanoparticles such as carbon nanotubes CNTs, graphene [17], nanodiamonds [18], and fullerenes [19], among others. They have been used as additives in different types of lubricants ranging from mineral [20] to vegetable oils [21,22]. In the vast majority of research papers, the addition of these nanoparticles significantly improved the performance of lubricants. Researchers have attributed this improvement to the different mechanisms of action that are at play: the rolling effect, where spherical and semi-spherical nanoparticles transform the mode of friction from sliding to a mixture of sliding and rolling [23]; the mending effect, where smaller-sized nanoparticles enter the grooves found on surfaces and mend them [24]; the tribofilm formation effect, where a protective layer is formed through either chemical reactions with the surface or the melting of the nanoparticles [25]; and the polishing effect, where the nanoparticles mechanically smoothen the surface by polishing the asperities found on it [26].

Carbon-based nanoparticles in particular have attracted the attention of researchers in several fields of study ranging from medicine [27], food and agriculture [28], and fuel cells [29] to water purification and treatment [30], among others. Their physical, chemical, and mechanical properties allow them to be used in a wide variety of applications; this also holds true for the field of tribology. These nanoparticles can be classified depending on their dimensionality, being zero-dimensional (0D), such as fullerenes, one-dimensional (1D), such as carbon nanotubes, two-dimensional (2D), such as graphene, or three-dimensional (3D), such as nanodiamonds [31,32]. Fullerenes have been studied by researchers and have shown impressive potential when used as nanoadditives. Lee et al. [33] conducted a study on the influence of fullerene nanoparticles on the performance of a mineral oil. The tests were carried out using a disk-on-disk tester, and the results showed that the optimal concentration of fullerene nanoparticles was 0.5 wt.%, which decreased the friction coefficient the most. The researchers also noted that with the increase in the concentration of the nanoparticles, the contacting surfaces became smoother, with lower peaks and shallower valleys. Another study by Ku et al. [34] looked at the effects of adding fullerene nanoparticles to oils of varying viscosities. The researchers noted the existence of a trend in which the increases in viscosity for both the nanofluid and raw oil led to a decrease in the WSD, and this decrease was much larger in the case of the nanofluid. The researchers also noted that the impact that the fullerene nanoparticles had on the oils regarding decreases in the coefficient of friction and WSD was much more pronounced and noticeable for oils with lower viscosities under higher loads. Carbon nanotubes have received increased attention from researchers because of their friction- and wear-reducing properties. Cornelio et al. [35] tested carboxylic acid-modified single-walled carbon nanotubes (SWCNTs) and multi-walled carbon nanotubes (MWCNTs) as additives in both oil and water. The results showed that using the carbon nanotubes (CNTs) decreased the coefficient of friction and the wear losses, with the lowest recorded coefficient of friction being 0.063. The optimal concentration of MWCNTs having the best performance in oil was determined to be 0.01 wt.%, while for water the best performing nanoparticles were the SWCNTs with the optimal concentration of 0.05 wt.%. The authors attributed the mechanism of action of these nanoparticles to the formation of an amorphous carbon film that protected the surfaces.

Another study by Bhaumik et al. [36] compared the effects of MWCNTs to that of graphite as nanoadditives to a mineral gear oil with a viscosity of 250 cSt. The study showed that the usage of MWCNTs provided better friction and wear reduction and that they were overall more efficient additives than graphite. The optimal MWCNT concentration was determined to be 0.5 wt.%, with concentrations above that reducing the lubricating properties of the oil. The authors attributed the mechanism of action of the MWCNTs to the rolling effect between the surfaces at low nanoparticle concentrations. A comprehensive study conducted by Nunn et al. [37] on the effects of different carbon-based nanoadditives showed favorable results. In that paper, the researchers used nanodiamonds, SWCNTs, MWCNTs, nanographene platelets, and onion-like carbon nanoparticles as additives in a PAO (Polyalphaolefin) base oil. The results showed that the nanodiamonds had by far the lowest coefficient of friction, which was a decrease of up to 70× that of the pure PAO oil with the optimal concentration being 0.01 wt.%. However, the wear from the usage of nanodiamonds was much more pronounced in comparison to the pure oil and the other nanoparticles, and the authors attributed this to the smoothing and polishing effect that the nanodiamonds have on the contacting surfaces. As for the rest, the MWCNTs performed the best in regard to wear and friction reduction with the nanographene platelets, showing an enhancement in the overall tribological performance of the base oil.

As can be seen, various studies have explored the effects that the addition of the different carbon-based nanoparticles has on the performance of lubricants. The mechanisms of their actions were proposed and verified by the results. However, the proposed mechanisms only encapsulate the effects that these nanoparticles have on the lubricant–surface interface. What has not been sufficiently explored are the mechanisms of interaction between the nanoparticles and the different components of the lubricant inside the lubricant film itself. In this regard, the aim of this paper is to study the effects of different carbon-based nanoadditives on the performance of a mineral oil, a vegetable oil, and an oil blend of the two and to see if there exists a synergistic effect inside the lubricant film between the nanoparticles and base oils. The nanoparticles in question are SWCNTs, SWCNT-COOH, fullerenes, and graphene. The tests were conducted to determine the welding point for each sample using a four-ball tester, and the coefficient of friction and wear scar diameter were determined using high-frequency reciprocating rig equipment (HFRR).

2. Materials and Methods

2.1. Lubricants

Two different base oils were considered for these series of tests: a mineral oil, SN150, provided by Lukoil Lubricants Romania, and a food-grade vegetable oil, rapeseed oil (RSO), that was obtained after the first press. The physical and chemical properties of the lubricants are highlighted in Table 1.

Table 1. Physical and chemical properties of the lubricants.

Properties	SN150	RSO	Blend	Methods
Density (20 °C, kg/m^3)	871.1	916.6	892.7	ASTM D-1298
Kinematic viscosity (40 °C, cSt)	30.49	35.97	31.59	ASTM D-445
Kinematic viscosity (100 °C, cSt)	5.18	8.01	6.4	ASTM D-445
Viscosity index	98	205	160	ASTM D-2270
Flash point (°C)	254	238	241	ASTM D-92
Pour point (°C)	−20	−24	−22	ASTM D-97
Copper corrosion (at 100 °C)	1a	1a	1a	ASTM D-130
Acid value (mgKOH/g)	0.12	2.7	1.8	ASTM D-974

Table 1. *Cont.*

Properties	SN150	RSO	Blend	Methods
Oxidation stability by RBOT, min	60	46	30	ASTM D-2272
Wear scar diameter according to 4 ball tester, µm (75 °C, 60 min, 1200 RPM, 147 N)	605.8	413.6	448.7	ASTM D-4172-94

2.2. Nanomaterials

Four carbon-based nanomaterials were used in the tests: fullerenes (C60, 99%), graphene platelets (6–8 nm, 99.5%), single-walled carbon nanotubes (SWCNTs) (OD < 2 nm, L < 20 µm, CNT > 90%, SWNT > 50%), and functionalized single-walled carbon nanotubes with a carboxyl group (SWCNT-COOH) (OD: 1–2 nm, L: 5–20 nm, CNT 90+%, SWCNT 60%, -COOH 5%), all of which were provided by Iolitec-ionic liquid technologies GmbH.

2.2.1. Characterization with XRD

Each nanomaterial was tested and characterized using XRD. XRD patterns were explored in a 2-theta range of 1–10° using a Bruker D8 instrument from Germany (λ = 0.154 nm, 40 kV, and 40 mA) with a CuK-α X-ray.

Figure 1 highlights the XRD profiles for each nanomaterial. Peaks at 2θ = 10.57°, 17.48°, 20.55°, 27.93°, 30.7°, and 32.6° were due to the C60 fullerene nanowhiskers, and were assigned to the (111), (220), (222), (420), (422), and (333) Miller index planes, respectively, while for graphene, peaks were identified corresponding to the (002) and (110) Miller index planes assigned to graphite sheets. For the SWCNTs and SWCNT-COOH, peaks corresponding to (002), (100), and (004) were identified, related to the hexagonal ring structure of graphite sheets forming the carbon nanotube. The crystallite sizes were calculated with Scherrer Equation (1), which gives a correspondence between the crystallite size (*LC*) and the full width of half maximum (*FWHM*):

$$LC = \frac{180}{\pi} \cdot \frac{k \cdot \lambda}{\cos \Theta \cdot \sqrt{FWHM^2 - s^2}}, \quad (1)$$

where k is the Scherrer constant (0.89), λ represents the wavelength of the radiation (1.54 Å), and s is the instrumental broadening (for our instrument is 0).

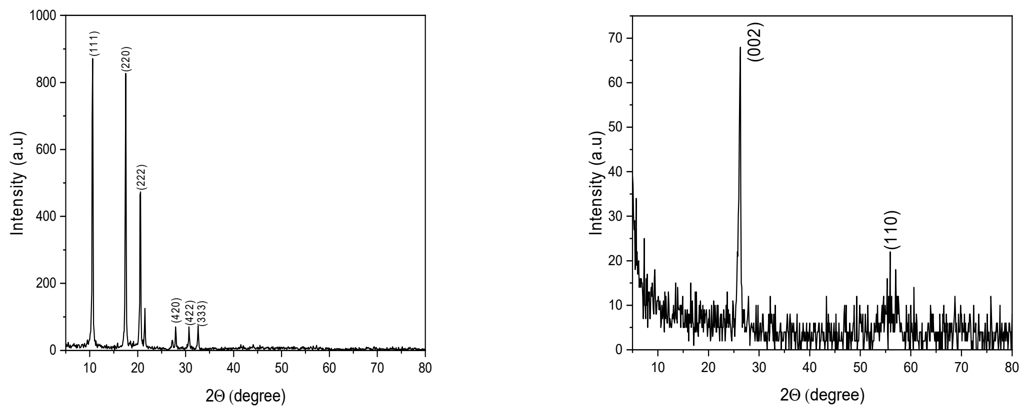

(**a**) (**b**)

Figure 1. *Cont.*

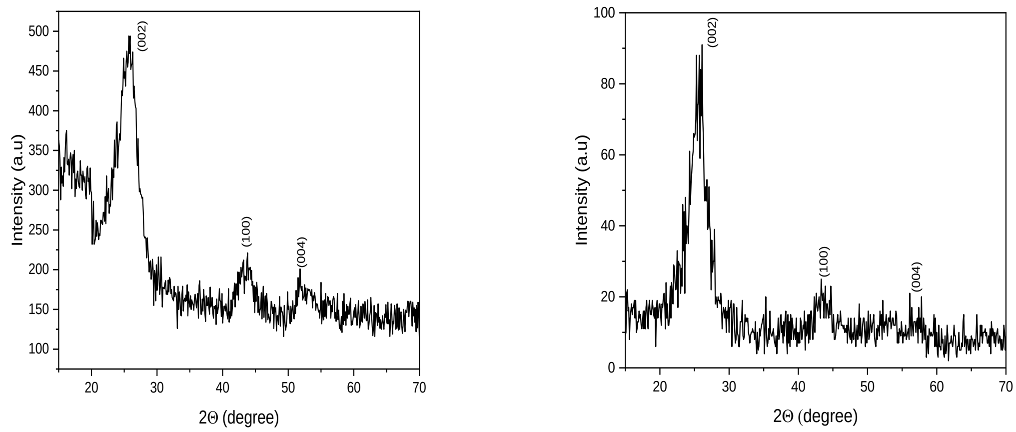

(**c**) (**d**)

Figure 1. (**a**) Graph showing XRD profiles of fullerenes; (**b**) graph showing XRD profiles of graphene; (**c**) graph showing XRD profiles of SWCNTs; (**d**) graph showing XRD profiles of SWCNT-COOH.

The crystallite sizes for fullerenes varied between 338 and 480 Å, for SWCNTs and SWCNT-COOH between 39 and 50 Å, and for graphene the calculated size was 237 Å.

2.2.2. Characterization with SEM

Figure 2 shows the microstructural morphologies of the samples. They were examined using a scanning electron microscope (SEM, Scios 2 HIVAC Dual-Beam ultra-high-resolution FIB-SEM; ThermoFisher, Brno, Czech Republic).

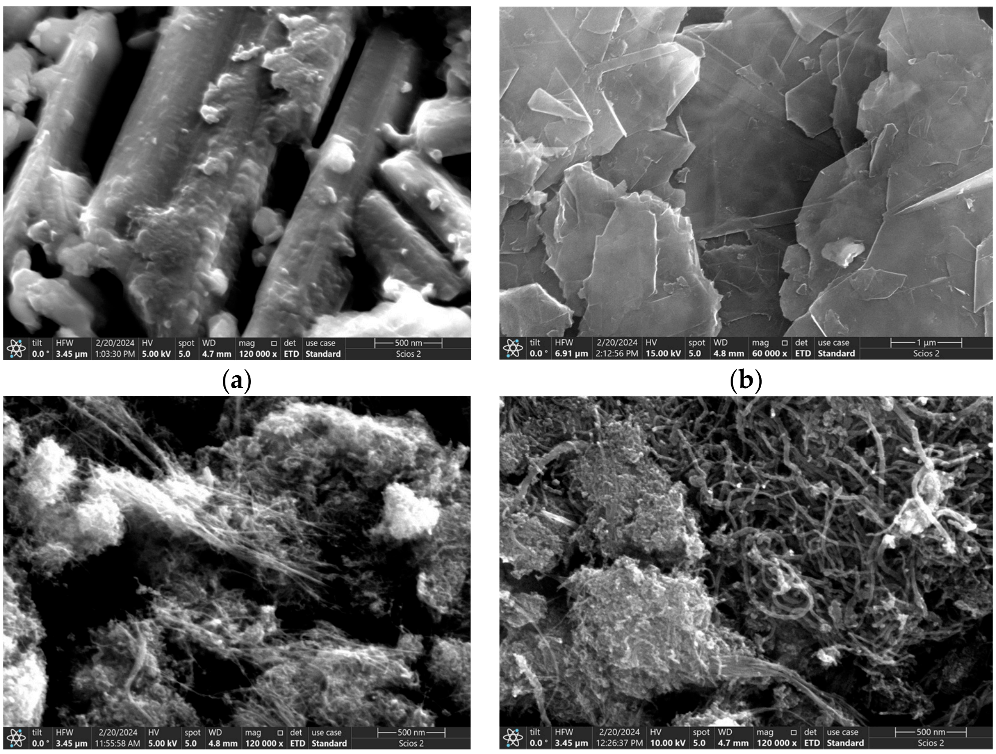

(**a**) (**b**)

(**c**) (**d**)

Figure 2. (**a**) Microstructural morphology of fullerenes; (**b**) microstructural morphology of graphene; (**c**) microstructural morphology of SWCNTs; (**d**) microstructural morphology of SWCNT-COOH.

2.3. Sample Preparation

For each oil- and carbon-based nanoparticle, 4 samples were prepared with different nanoparticle concentrations: 0.1, 0.5, 1, and 2 wt.%. A 50/50 by volume oil blend of the two base oils was prepared and tested as well. The samples were split into 3 different groups: group I comprised seventeen samples, the pure base mineral oil SN150 and the samples of the different nanofluids formulated with the addition of the carbon-based nanoparticles with their different concentrations. Group II comprised the pure vegetable oil, rapeseed oil, and the four samples formulated with the addition of the different nanoparticle concentrations. And finally, group III comprised the pure 50/50 by volume blend and the samples formulated with the nanoparticles. In total, 51 samples were prepared and then tested using the HFRR in order to compare the performance of the pure oil samples and the addition of the carbon-based nanoparticles.

As for the welding point tests, 15 samples were prepared; those included the pure oils, the pure oil blend, and the nanofluids formulated with the addition of 0.5 wt.% of the nanoparticles.

2.4. HFRR Test Setup

The samples were tested using the HFRR (Model PCS-002817) in order to determine the effects of the addition of different nanomaterials on the performance of the oils in regard to the coefficient of friction and wear scar diameter. The HFRR tests the performance of a given oil sample by rubbing a steel ball (AISI-E 52100/535A99 with 6 mm diameter, roughness Ra = 0.050 μm, hardness RC 58–66) against a steel disk (AISI-E 52100/535A99 with 10 mm diameter, roughness Ra = 0.020 μm, hardness RC 76–79) under the set test conditions. These tests were conducted under the following conditions: a stroke of 1000 μm, a frequency of 50 Hz, a load of 400 g, a temperature of 25 °C, and a duration of 60 min. Before each test, each nanofluid sample was sonicated for 25 min using an ultrasonication bath that was held at 60 °C. Then, the samples were added to the HFRR tester and allowed to reach the set test temperature and the tests were conducted. The HFRR allows the continuous recording of the COF throughout each test and provides the average COF at the end of them. After each test was completed, the ball was cleaned using acetone and was put under an optical microscope in order to determine the WSD present on it for each tested sample. Each test was repeated 2 additional times in order to validate the obtained results.

2.5. Welding Point Test Setup

The welding point of each oil sample was determined using a four-ball tester according to test standards [38]. A series of 10 s tests with increasing loads and a rotational speed of 1760 rpm was conducted until welding occurred. The initial load that the system was subjected to was 80 kgf (784.5 N). The nanofluid samples used had a nanoparticle concentration of 0.5 wt.%. Similarly to the HFRR tests, before each welding point test, the nanofluid samples were sonicated for 25 min.

3. Results

3.1. HFRR Tests

3.1.1. Mineral Oil Samples

The tests conducted on the SN150 samples yielded the following results.

Regarding the COF, compared to the pure SN150 sample for which the test recorded an average COF of 0.081, only four other samples performed better: the 1 and 2 wt.% of fullerenes and SWCNT-COOH, with each recording 0.08 and 0.076 for the fullerenes and 0.078 and 0.077 for the SWCNT-COOH, respectively. The results are summarized in Table 2 and Figure 3.

Table 2. HFRR test results for SN150 samples with different nanoparticles.

Nanoparticle	Nanoparticle Concentration wt.%							
	COF				WSD (μm)			
	0.1	0.5	1	2	0.1	0.5	1	2
SWCNT-COOH	0.084	0.086	0.078	0.077	171	169	195	173
SWCNTs	0.088	0.09	0.09	0.093	171	176	186	178
Fullerenes	0.081	0.084	0.08	0.076	126	118	137	158
Graphene	0.082	0.092	0.094	0.094	112	130	174	226

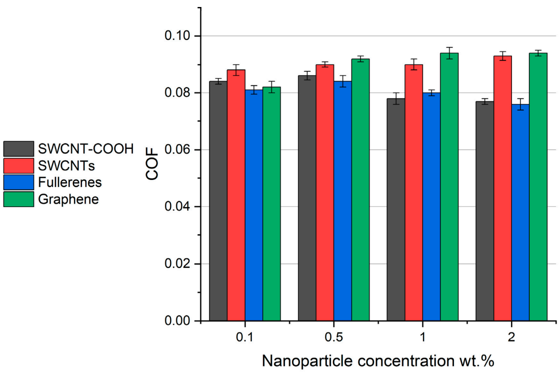

(**a**)

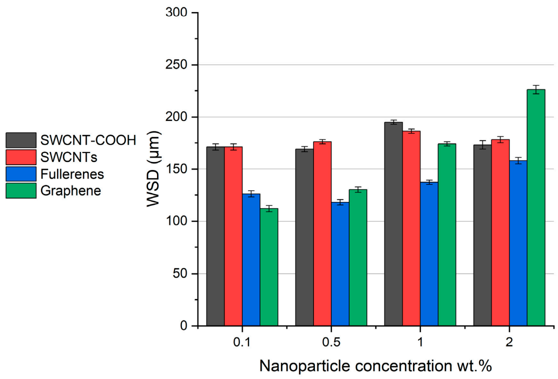

(**b**)

Figure 3. (**a**) Graph showing the COF results for the different nanofluid samples with SN150; (**b**) graph showing the WSD results for the different nanofluid samples with SN150.

Concerning the WSD, for the pure SN150 sample, it was measured to be 116 μm. Comparatively, the only sample for which the WSD was lower than the pure SN150 sample was the 0.1 wt.% of graphene. Figure 4 shows the resulting wear from the test conducted with this sample.

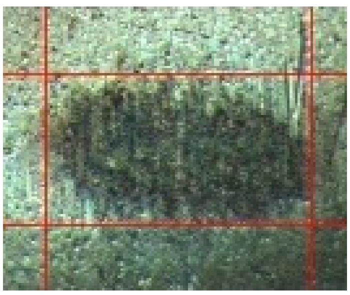

Figure 4. Optical micrograph of the WSD for the SN150 + 0.1 wt.% graphene sample.

3.1.2. Vegetable Oil Samples

The tests conducted on the RSO samples yielded the following results.

Regarding the COF, the improvement was more noticeable with the addition of the different nanoparticle concentrations. While the pure RSO sample recorded a COF of 0.064, all four SWCNT-COOH samples recorded an improvement, with 0.5 wt.% being the best among them with a COF of 0.054. Similarly, the addition of fullerenes improved the performance of the RSO, with the addition of 1 wt.% being the best performing sample with a COF of 0.049. Both the SWCNTs and graphene improved the performance of the RSO at lower concentrations, with 0.1 wt.% being the optimal concentration for both with the COFs being 0.057 and 0.058, respectively. Table 3 summarizes the results obtained from the tests conducted on the RSO samples.

Table 3. HFRR test results for RSO samples with different nanoparticles.

Nanoparticle	Nanoparticle Concentration wt.%							
	COF				WSD (μm)			
	0.1	0.5	1	2	0.1	0.5	1	2
SWCNT-COOH	0.059	0.054	0.059	0.063	185	155	173	160
SWCNTs	0.057	0.066	0.064	0.065	201	185	255	184
Fullerenes	0.067	0.054	0.049	0.054	194	155	142	170
Graphene	0.058	0.06	0.068	0.067	165	212	259	250

As for the WSD, it was measured to be 151.5 μm for the pure RSO sample. The only sample from this group that outperformed it was the 1 wt.% of fullerenes, whose WSD was measured to be 142 μm. Figure 5 showcases how the results from the tests conducted on the RSO samples compared to one another.

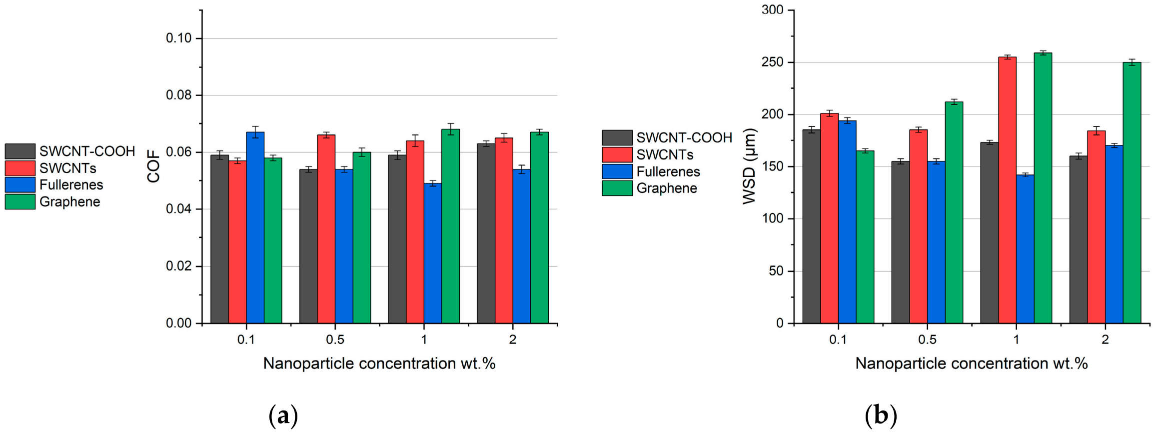

Figure 5. (**a**) Graph showing the COF results for the different nanofluid samples with RSO; (**b**) graph showing the WSD results for the different nanofluid samples with RSO.

3.1.3. Oil Blend Samples

The test conducted on the oil blend samples yielded the following results.

Regarding the COF, all SWCNT-COOH and fullerene samples recorded COFs that were equal to or less than that of the pure oil blend sample, whose recorded COF was 0.071. Comparatively, all SWCNT and graphene samples recorded COFs that were equal to or worse than that of the pure oil blend. The results are summarized in Table 4.

Table 4. HFRR test results for oil blend samples with different nanoparticles.

Nanoparticle	Nanoparticle Concentration wt.%							
	COF				WSD (μm)			
	0.1	0.5	1	2	0.1	0.5	1	2
SWCNT-COOH	0.064	0.071	0.06	0.067	120	136	134	145
SWCNTs	0.079	0.073	0.072	0.071	175	220	283	307
Fullerenes	0.066	0.064	0.071	0.066	131	120	135	122
Graphene	0.073	0.079	0.08	0.08	224	159	186	218

In terms of the WSD, similarly to the COF, noticeable improvements were observed with the addition of different SWCNT-COOH and fullerene concentrations compared to the pure oil blend sample, whose WSD was measured to be 168 μm. As for the SWCNTs, the WSD was increased compared to the pure oil blend sample for all tested concentrations. For graphene, 0.5 wt.% was shown to be the best concentration, for which the WSD was measured to be 159 µm. Figure 6 shows how the results from the oil blend samples compare to one another, while Figure 7 shows the resulting wear from one of the better performing samples.

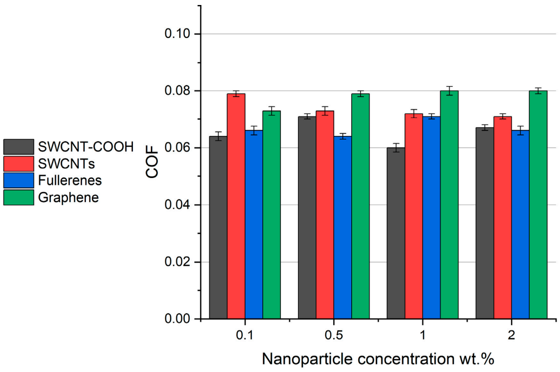

(**a**)

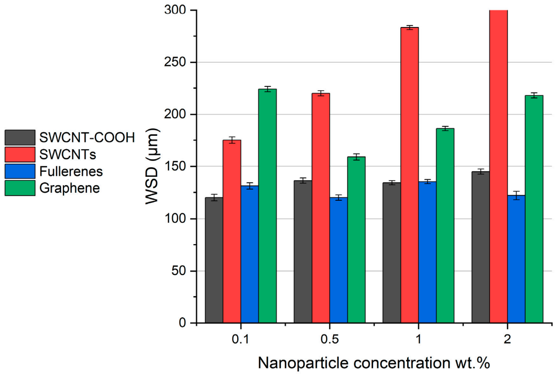

(**b**)

Figure 6. (**a**) Graph showing the COF results for the different nanofluid samples with the oil blend; (**b**) graph showing the WSD results for the different nanofluid samples with the oil blend.

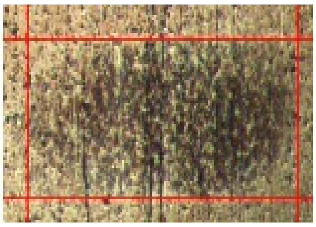

Figure 7. Optical micrograph of the WSD for the blend + 1 wt.% SWCNT-COOH sample.

3.2. Welding Point Tests

The results of the welding point tests conducted on the different samples show a very clear image; the addition of the different nanoparticles decreased the welding point for each oil sample. While the pure RSO had a much higher welding point than the pure SN150, welding occurred at the same applied force of 360 kgf (3530.3 N) for the oil blend as for the pure SN150. The results from the welding point tests are summarized in Table 5.

Table 5. Welding point test results for the different samples.

Lubricant	Force (N)				
	Pure	**Graphene**	**Fullerenes**	**SWCNTs**	**SWCNT-COOH**
SN150	3530.3	1372.9	1274.8	1569	1569
RSO	4707.1	2745.8	1765.1	2353.5	1765.1
50-50 Oil Blend	3922.6	1765.1	1765.1	1765.1	3530.3

4. Discussion

The results obtained from the HFRR tests can be attributed to different mechanisms and interactions that were occurring inside the lubrication system between its different components.

When comparing the performance of the different pure oil samples, such as in Figure 8, Figure 9, and Table 6, it is evident that in terms of the COF, the pure RSO outperforms both the SN150 and the blend. This is due to the enhanced lubricity that vegetable oils are known for. Vegetable oils are mainly composed of triglycerides and fatty acids whose polar heads gravitate towards metal surfaces, allowing their non-polar tails to form a densely packed molecular layer that protects their surfaces [39].

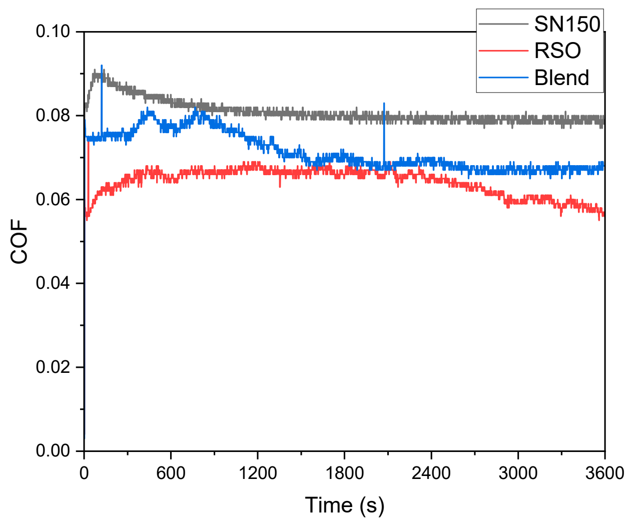

Figure 8. Graph of the COF vs. time data recorded during the tests for the different neat lubricants.

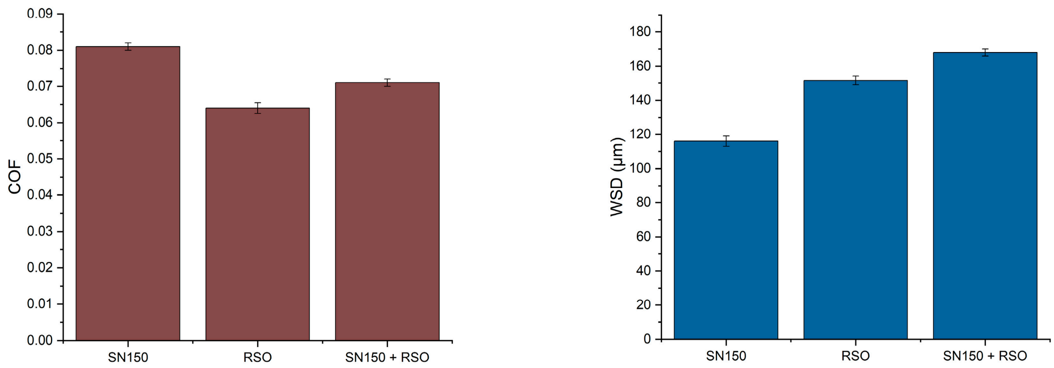

(**a**) (**b**)

Figure 9. (**a**) Graph showing the COF results for the different pure oil samples; (**b**) graph showing the WSD results for the different pure oil samples.

Table 6. HFRR test results for the pure oil samples.

Lubricant	COF	WSD (μm)
SN150	0.081	116
RSO	0.064	151.5
50-50 Oil Blend	0.071	168

When comparing the performance of the SWCNTs and the SWCNT-COOH, the results showed that the SWCNT-COOH outperformed the SWCNTs, especially in both the RSO and oil blend. This is due to the agglomeration that carbon-based nanoparticles in general experience due to the strong van der Waals forces that exist between each particle [40]. This has been shown to be mitigated by functionalizing them [41–43], as was the case with the SWCNT-COOH, with the presence of the carboxyl group ensuring a more even dispersion of the nanoparticles in the oils. This shows that the tendency of these nanoparticles to agglomerate hinders their performance and that functionalization as well as choosing the adequate carrier oil for these nanoparticles can help improve the overall performance of the oil.

When comparing the results of the SWCNT-COOH and fullerenes between the different oils, it can be seen that their addition to the oil blend had the highest impact and improved its performance to levels comparable to the pure oils, if not better. Figure 10 is an example of this, as the addition of the fullerene nanoparticles significantly impacted the blend more so than the other lubricants. This shows that there might exist a synergistic effect between certain nanoparticles and oil blends. The nanoparticles could be influencing the interactions of the different lubricant molecules inside the lubricant film. It has been suggested that the presence of nanoparticles can influence the flow of lubricant molecules inside the lubricant film and make it so that they are less likely to collide and cause internal friction [44]. Another possible explanation is that the presence of the nanoparticles with their small sizes allows them to enter the regions between the lubricant molecules. As such, the nanoparticles helped consolidate the molecular layers that formed, making it so that the lubricant film is less likely to deteriorate while decreasing the internal friction that arises from the collisions between the different lubricant molecules.

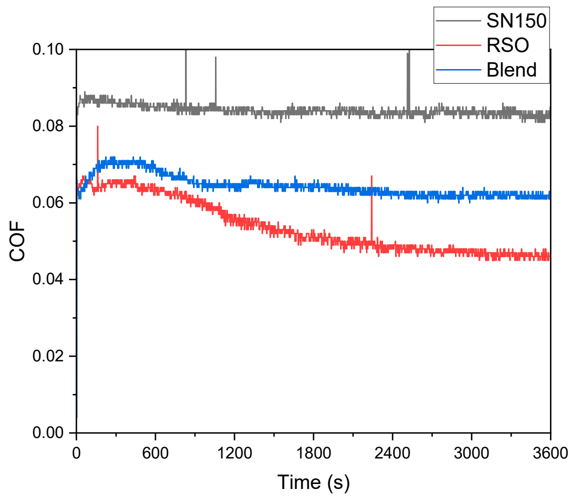

Figure 10. Graph of the COF vs. time data recorded during the tests for the lubricants with the addition of 0.5 wt.% fullerenes.

Finally, it can be observed that for each nanoparticle, a different optimal concentration exists for which its effect on both the COF and the WSD are most pronounced. This optimal concentration varies for each nanoparticle and for each oil it is added to, and concentrations below or above it do not provide as substantial of an effect on the performance as it does.

As for the welding point test results, the hardness of the nanoparticles plays a significant role, especially when these specific nanoparticles do not react with the surfaces to create a protective tribofilm like metals and metal oxides do. What is believed to have occurred was that at such high pressures that the system was subjected to, the local pressure and temperature at the contact points between the surfaces and the nanoparticles were significantly increased, causing welding to occur earlier compared to the pure oils.

5. Conclusions

The performance of different carbon-based nanoparticles as additives in three types of oils, mineral, vegetable, and a blend of the two, was tested using an HFRR and a four-ball tester. The welding point test results showed that the addition of these nanoparticles ensures that welding occurs much earlier compared to the pure base oils; this is due to the increased local pressure and temperature at the points of contact between the surfaces and the nanoparticles. As for the HFRR tests, the results showed that functionalized SWCNTs with a carboxyl group perform better than pure SWCNTs, especially in the RSO and the oil blend. The authors attribute this to the ability of the SWCNT-COOH to disperse much better and more evenly inside the carrier oil compared to the pure SWCNTs. The results also showed that different nanoparticles have different optimal concentrations depending on the oil they are added to. This particular oil blend of 50/50 by volume of SN150 and RSO shows promise, especially with the addition of fullerenes and SWCNT-COOH, with the results showing a possible synergistic effect. This could be the result of an interaction between the nanoparticles and the lubricant molecules, where it has been proposed that the nanoparticles could influence the flow pattern of the lubricant molecules, thereby reducing the internal friction. In addition, the presence of these nanoparticles could help consolidate the lubricant molecular layers that protect the surfaces. These results show that oil blends have the potential to play a bigger role in the future and that the interactions between nanoadditives and lubricant molecules should be the subject of future research in order to understand the different mechanisms at play.

Author Contributions: Conceptualization, J.N. and D.-L.C.; methodology, J.N. and D.-L.C.; validation, J.N. and D.-L.C.; formal analysis, J.N.; investigation, J.N.; resources, D.-L.C.; data curation, J.N.; writing—original draft preparation, J.N.; writing—review and editing, D.-L.C.; visualization, J.N.; supervision, D.-L.C.; project administration, D.-L.C. All authors have read and agreed to the published version of the manuscript.

Funding: This research received no external funding.

Data Availability Statement: Data are contained within the article.

Conflicts of Interest: The authors declare no conflicts of interest.

References

1. Nowak, P.; Kucharska, K.; Kamiński, M. Ecological and Health Effects of Lubricant Oils Emitted into the Environment. *Int. J. Environ. Res. Public Health* **2019**, *16*, 3002. [CrossRef]
2. Jayadas, N.H.; Nair, K.P.; Ajithkumar, G. Tribological Evaluation of Coconut Oil as an Environment-Friendly Lubricant. *Tribol. Int.* **2007**, *40*, 350–354. [CrossRef]
3. Rani, S.; Joy, M.L.; Nair, K.P. Evaluation of Physiochemical and Tribological Properties of Rice Bran Oil—Biodegradable and Potential Base Stoke for Industrial Lubricants. *Ind. Crops Prod.* **2015**, *65*, 328–333. [CrossRef]
4. Kalam, M.A.; Masjuki, H.H.; Cho, H.M.; Mosarof, M.H.; Mahmud, M.I.; Chowdhury, M.A.; Zulkifli, N.W.M. Influences of Thermal Stability, and Lubrication Performance of Biodegradable Oil as an Engine Oil for Improving the Efficiency of Heavy Duty Diesel Engine. *Fuel* **2017**, *196*, 36–46. [CrossRef]
5. Quinchia, L.A.; Delgado, M.; Franco, J.M.; Spikes, H.A.; Gallegos, C. Low-Temperature Flow Behaviour of Vegetable Oil-Based Lubricants. *Ind. Crops Prod.* **2012**, *37*, 383–388. [CrossRef]
6. Hamnas, A.; Unnikrishnan, G. Bio-Lubricants from Vegetable Oils: Characterization, Modifications, Applications and Challenges—Review. *Renew. Sustain. Energy Rev.* **2023**, *182*, 113413. [CrossRef]
7. Merrill, L.I.; Pike, O.A.; Ogden, L.V.; Dunn, M.L. Oxidative Stability of Conventional and High-Oleic Vegetable Oils with Added Antioxidants. *J. Am. Oil Chem. Soc.* **2008**, *85*, 771–776. [CrossRef]
8. Asadauskas, S.; Perez, J.M.S.; Duda, J.L. Oxidative Stability and Antiwear Properties of High Oleic Vegetable Oils. *Lubr. Eng.* **1996**, *52*, 877–882.
9. Singh, Y. Tribological Behavior as Lubricant Additive and Physiochemical Characterization of Jatropha Oil Blends. *Friction* **2015**, *3*, 320–332. [CrossRef]
10. Basiron, J.; Abdollah, M.F.B.; Abdullah, A.S.; Amiruddin, H. Lubricant Mechanisms of Eco-Friendly Lubricant Blended with Mineral Oil for Steel-Steel Contact. *Tribol. Int.* **2023**, *186*, 108653. [CrossRef]
11. Bahari, A.; Lewis, R.; Slatter, T. Friction and Wear Response of Vegetable Oils and Their Blends with Mineral Engine Oil in a Reciprocating Sliding Contact at Severe Contact Conditions. *Proc. Inst. Mech. Eng. Part J J. Eng. Tribol.* **2017**, *232*, 244–258. [CrossRef]
12. Alam, I.; Masjuki, H.H.; Kalam, M.A.; Varman, M.; Hasmelidin, M.; Mahmud, K.A.H.A.; Shahir, S.A.; Habibullah, M. Study of Friction and Wear Characteristic of Jatropha Oil Blended Lube Oil. *Procedia Eng.* **2013**, *68*, 178–185.
13. Yu, H.; Xu, Y.; Shi, P.-J.; Xu, B.; Wang, X.; Liu, Q. Tribological Properties and Lubricating Mechanisms of Cu Nanoparticles in Lubricant. *Trans. Nonferrous Met. Soc. China* **2008**, *18*, 636–641. [CrossRef]
14. Kumara, C.; Luo, H.; Leonard, D.N.; Meyer, H.M.; Qu, J. Organic-Modified Silver Nanoparticles as Lubricant Additives. *ACS Appl. Mater. Interfaces* **2017**, *9*, 37227–37237. [CrossRef] [PubMed]
15. Peña-Parás, L.; Taha-Tijerina, J.; La Garza, L.M.-D.; Maldonado-Cortés, D.; Michalczewski, R.; Lapray, C. Effect of CuO and Al_2O_3 Nanoparticle Additives on the Tribological Behavior of Fully Formulated Oils. *Wear* **2015**, *332–333*, 1256–1261. [CrossRef]
16. Battez, A.H.; González, R.; Viesca, J.L.; Fernández, J.M.V.; Fernández, J.; Machado, A.S.; Chou, R.; Riba, J. CuO, ZrO_2 and ZnO Nanoparticles as Antiwear Additive in Oil Lubricants. *Wear* **2008**, *265*, 422–428. [CrossRef]
17. Del Río, J.M.L.; Pérez, G.; Martínez, A.; Peña, D.; Fernández, J. Tribological Improvement of Potential Lubricants for Electric Vehicles Using Double Functionalized Graphene Oxide as Additives. *Tribol. Int.* **2024**, *193*, 109402. [CrossRef]
18. Piya, A.K.; Yang, L.; Omar, A.A.S.; Emami, N.; Morina, A. Synergistic Lubrication Mechanism of Nanodiamonds with Organic Friction Modifier. *Carbon* **2023**, *218*, 118742. [CrossRef]

19. Dai, Y.; Feng, X.; Liu, Y.; Huang, J.; Wu, S.; Zhou, P.; Li, H. Onion-like Carbon Nanoparticles as Additives in Lubricant Oil Deform Inelastically during the Wear Testing for Improved Lubrication Performances. *Mater. Chem. Phys.* **2024**, *314*, 128836. [CrossRef]
20. Wang, X.L.; Yin, Y.; Zhang, G.N.; Wang, W.Y.; Zhao, K. Study on Antiwear and Repairing Performances about Mass of Nano-Copper Lubricating Additives to 45 Steel. *Phys. Procedia* **2013**, *50*, 466–472. [CrossRef]
21. Saravanakumar, N.; Saravanan, M.L.J.; Barathkumar, K.E.; Kannan, K.; Karthikeyan, R. Development and Testing of Nano Particulate Lubricant for Worm Gear Application. *J. Mech. Sci. Technol.* **2019**, *33*, 1785–1791. [CrossRef]
22. Gupta, R.; Harsha, A.P. Tribological Study of Castor Oil with Surface-Modified CuO Nanoparticles in Boundary Lubrication. *Ind. Lubr. Tribol.* **2018**, *70*, 700–710. [CrossRef]
23. Guo, D.; Luo, J. Mechanical Properties of Nanoparticles: Basics and Applications. *J. Phys. D Appl. Phys.* **2013**, *47*, 013001. [CrossRef]
24. Srinivas, V.; Thakur, R.N.; Jain, A.K. Antiwear, Antifriction, and Extreme Pressure Properties of Motor Bike Engine Oil Dispersed with Molybdenum Disulfide Nanoparticles. *Tribol. Trans.* **2016**, *60*, 12–19. [CrossRef]
25. Padgurskas, J.; Rukuiža, R.; Prosyčevas, I.; Kreivaitis, R. Tribological Properties of Lubricant Additives of Fe, Cu and Co Nanoparticles. *Tribol. Int.* **2013**, *60*, 224–232. [CrossRef]
26. Rahmati, B.; Sarhan, A.A.D.; Sayuti, M. Morphology of Surface Generated by End Milling AL6061-T6 Using Molybdenum Disulfide (MoS_2) Nanolubrication in End Milling Machining. *J. Clean. Prod.* **2014**, *66*, 685–691. [CrossRef]
27. Liu, Y.; Liu, H.; Guo, S.; Zhao, Y.; Qi, J.; Zhang, R.; Ren, J.; Cheng, H.; Zong, M.; Wu, X.; et al. A Review of Carbon Nanomaterials/Bacterial Cellulose Composites for Nanomedicine Applications. *Carbohydr. Polym.* **2024**, *323*, 121445. [CrossRef]
28. Mishra, S.; Mishra, S.; Patel, S.S.; Singh, S.P.; Kumar, P.; Khan, M.A.; Awasthi, H.; Singh, S. Carbon Nanomaterials for the Detection of Pesticide Residues in Food: A Review. *Environ. Pollut.* **2022**, *310*, 119804. [CrossRef]
29. Haque, S.U.; Nasar, A.; Duțeanu, N. Inamuddin Carbon Based-Nanomaterials Used in Biofuel Cells—A Review. *Fuel* **2023**, *331*, 125634. [CrossRef]
30. Zhang, Y.; Luo, J.; Zhang, H.; Li, T.; Xu, H.; Sun, Y.; Gu, X.; Hu, X.; Gao, B. Synthesis and Adsorption Performance of Three-Dimensional Gels Assembled by Carbon Nanomaterials for Heavy Metal Removal from Water: A Review. *Sci. Total Environ.* **2022**, *852*, 158201. [CrossRef]
31. Shahnazar, S.; Bagheri, S.; Hamid, S.B.A. Enhancing Lubricant Properties by Nanoparticle Additives. *Int. J. Hydrogen Energy* **2016**, *41*, 3153–3170. [CrossRef]
32. Rahman, M.M.; Islam, M.; Roy, R.; Younis, H.; AlNahyan, M.; Younes, H. Carbon Nanomaterial-Based Lubricants: Review of Recent Developments. *Lubricants* **2022**, *10*, 281. [CrossRef]
33. Lee, J.-K.; Cho, S.; Hwang, Y.; Lee, C.-G.; Kim, S.H. Enhancement of Lubrication Properties of Nano-Oil by Controlling the Amount of Fullerene Nanoparticle Additives. *Tribol. Lett.* **2007**, *28*, 203–208. [CrossRef]
34. Ku, B.; Han, Y.; Lee, J.-E.; Lee, J.-K.; Park, S.-H.; Hwang, Y. Tribological Effects of Fullerene (C60) Nanoparticles Added in Mineral Lubricants According to Its Viscosity. *Int. J. Precis. Eng. Manuf.* **2010**, *11*, 607–611. [CrossRef]
35. Cornelio, J.A.C.; Cuervo, P.; Palacio, L.M.H.; Lara-Romero, J.; Toro, A. Tribological Properties of Carbon Nanotubes as Lubricant Additive in Oil and Water for a Wheel–Rail System. *J. Mater. Res. Technol.* **2016**, *5*, 68–76. [CrossRef]
36. Bhaumik, S.; Prabhu, S.; Singh, D.K.J. Analysis of Tribological Behavior of Carbon Nanotube Based Industrial Mineral Gear Oil 250 CSt Viscosity. *Adv. Tribol.* **2014**, *2014*, 341365. [CrossRef]
37. Nunn, N.; Mahbooba, Z.; Ivanov, M.G.; Ivanov, D.M.; Brenner, D.W.; Shenderova, O. Tribological Properties of Polyalphaolefin Oil Modified with Nanocarbon Additives. *Diam. Relat. Mater.* **2015**, *54*, 97–102. [CrossRef]
38. *ASTM D2783-03*; Measurement of Extreme-Pressure Properties of Lubricating Fluids (Four-Ball Method). ASTM International: West Conshohocken, PA, USA, 2009.
39. Huang, W.; Tan, Y.; Chen, B.; Dong, J.; Wang, X. The Binding of Antiwear Additives to Iron Surfaces: Quantum Chemical Calculations and Tribological Tests. *Tribol. Int.* **2003**, *36*, 163–168. [CrossRef]
40. Leang, T.J.; Walvekar, R.; Nagarajan, T.; Said, Z.; Khalid, M.; Mubarak, N.M. A Review on the Properties and Tribological Performance of Recent Non-Aqueous Miscible Lubricants. *J. Mol. Liq.* **2022**, *366*, 120274.
41. Lin, J.; Wang, L.; Chen, G. Modification of Graphene Platelets and Their Tribological Properties as a Lubricant Additive. *Tribol. Lett.* **2010**, *41*, 209–215. [CrossRef]
42. Zhang, W.; Zhou, M.; Zhu, H.; Tian, Y.; Wang, K.; Wei, J.; Ji, F.; Li, X.; Li, Z.; Zhang, P.; et al. Tribological Properties of Oleic Acid-Modified Graphene as Lubricant Oil Additives. *J. Phys. D Appl. Phys.* **2011**, *44*, 205303. [CrossRef]
43. Chen, C.S.; Chen, X.H.; Xu, L.; Liu, Y.; Li, W.H. Modification of Multi-Walled Carbon Nanotubes with Fatty Acid and Their Tribological Properties as Lubricant Additive. *Carbon* **2005**, *43*, 1660–1666. [CrossRef]
44. Ghaednia, H.; Babaei, H.; Jackson, R.L.; Bozack, M.J.; Khodadadi, J.M. The Effect of Nanoparticles on Thin Film Elasto-Hydrodynamic Lubrication. *Appl. Phys. Lett.* **2013**, *103*, 263111. [CrossRef]